Available online at www.sciencedirect.com
SCIENCE DIRECT®
Coordination Chemistry Reviews 248 (2004) 1501–1509
COORDINATION CHEMISTRY REVIEWS
www.elsevier.com/locate/ccr

Review

# A system approach to molecular solar cells

Anders Hagfeldt*, Gerrit Boschloo, Henrik Lindström, Egbert Figgemeier, Anna Holmberg, Viviane Aranyos, Eva Magnusson, Lennart Malmqvist

*Ångström Solar Center, Department of Physical Chemistry, Uppsala University, Box 579, 751 23 Uppsala, Sweden*

Received 11 February 2004; accepted 20 April 2004
Available online 2 July 2004

## Contents



## Abstract

This paper gives an overview of the research and development of dye-sensitized solar cells (DSC) within the Swedish research program ‘Ångström Solar Center’. A path towards low production cost is the development of a continuous process, which allows the production of solar cells in large volumes and with a high productivity. We have developed a deposition method for the production of the mesoporous $TiO_2$ electrode layer that is based on compression of a powder film at room temperature. This technique allows us to use flexible substrates—a prerequisite for a continuous process. A novel interconnect technology, compatible with a continuous production process, is described. Stability data of plastic DSC, exposed to indoor light for more than 10,000 h, demonstrates the possibility for the technology to be explored for various types of indoor applications.

Optimization of the DSC is a challenging task as it is a complex highly interacting molecular system. A system approach is proposed, where the complete DSC is investigated with a series of measurement techniques (‘toolbox’) that allows the study of the internal processes under relevant conditions. Two examples of such techniques are given.


*Keywords:* Dye-sensitized solar cells; Continuous production process; DSC system

## 1. Introduction

The unexpected discovery of a new type of solar cell based on dye-sensitized mesoporous oxide films by Prof. Michael Grätzel and co-workers [1,2] has had an enormous impact on research and development activities in various fields. The conventional solid-state photovoltaic technologies are now challenged by devices functioning on a molecular level [3]. Efficiencies above 10% and impressive stability data, passing for example the critical 1000 h stability test at 80 °C [4], have been accomplished.

The traditional solid-state view of photovoltaic materials is that pure, preferably single-crystal, semiconductor

* Corresponding author. Tel.: +46 18 47 13654.
*E-mail address:* anders.hagfeldt@fki.uu.se (A. Hagfeldt).

0010-8545/$ – see front matter © 2004 Elsevier B.V. All rights reserved.
doi:10.1016/j.ccr.2004.04.012

films are needed. Any type of defects in the material leads to recombination losses. With the breakthrough of the dye-sensitized solar cell (DSC), the scene is radically changed, technically as well as scientifically. The prospect of low-cost fabrication is a key feature. But also the possibilities for design of solar cell devices by the use of different material combinations, and the use of flexible plastic substrates, opens up new commercial opportunities.

From a basic science aspect we are also offered an intriguing system to investigate. The research is interdisciplinary, involving electrochemistry, semiconductor physics, surface physics and chemistry, materials science aspects in organic and inorganic chemistry, etc. It is a complex highly interacting system and the function of the system as a whole is larger than the sum of the components. A main scientific challenge is thus to create an understanding on how the simultaneous interactions between the different components build up a complex functioning DSC system.

The discovery of the DSC by Grätzel and co-workers have also inspired the development of other types of solar cells such as conducting polymer solar cells and extremely thin absorber (ETA) cells. Several spin-off applications based on mesoporous oxides have also been explored, for example, electrochromic displays [5,6], secondary Li-batteries [7], and photocatalysis [8].

In order to become viable within large scale solar cell production, the DSC has to deliver similar efficiencies and stability as thin films solar cells, however, at a significantly lower production cost. Two concepts lay the ground for our work to achieve these goals; a continuous production process and the analysis of dye-sensitized solar cells using a system approach. In this paper, we summarize our activities within the framework of these two concepts.Our main activities have been conducted within a national program called Ångström Solar Center. The Ångström Solar Center (ÅSC) is an R&D program for solar energy technologies. It includes thin film solar cells (CIGS), DSC solar cells and electrochromic “smart windows”. ÅSC started its activities in the fall of 1996. The overall objective of the program is to develop these technologies to a stage where the results can be handed over for a further industrial development.

## 2. Towards a continuous production process

The path towards a low production cost was identified early within the Ångström Solar Center program as a continuous process, which allows the production of solar cells in large volumes and with a high productivity. A prerequisite for a continuous web based process is the use of a flexible substrate. The most straightforward material is some type of polymer that can be rolled up. When using low-cost polymers as the substrate for the cells or modules, high temperatures in the manufacturing process cannot be accepted. Our concept for the production of the porous electrode layer at room temperature is to apply a pressure on the deposited $TiO_2$—the compression technique [9–11]. This technique allows us to use flexible substrates. We note that other groups have developed alternative low-temperature techniques for the deposition of $TiO_2$ on flexible substrates [12–14].

### 2.1. Preparation of mesoporous oxide films at room temperature

For preparation of the photoanode a suitable suspension is prepared by mixing $TiO_2$ powder (P25 from Degussa) together with a volatile solvent like, e.g. ethanol or water [10]. The composition of the P25-suspension has to be adjusted such that the deposition results in smooth and homogenous powder films. Using a solvent with low surface tension like, e.g. ethanol, will give an even smoother film deposition. A thin suspension layer is then deposited onto the conducting plastic substrate, e.g. ITO deposited on PET.

After the deposition of the film, the solvent is allowed to evaporate in air under ambient conditions. Depending on the thickness of the deposited layer and the solvent used, the evaporation process is normally completed within a few minutes. The resulting powder film is strongly light scattering and has poor intrinsic mechanical stability and can therefore be removed easily from the substrate by, e.g. scratching. Also, depending on the thickness of the deposited suspension layer, macroscopic cracks are formed to varying extents. Typically, for thicker suspension films, i.e. above 200 μm, macroscopic cracks in the powder film can be seen by visual inspection. However, when the thickness of the deposited layer was decreased, both the tendency of cracking decreased and the size of the cracks becomes smaller. It should be noted that although the powder film contains cracks, the adherence to the substrate is good and the substrate with the deposited film can therefore easily be handled without peeling off during transport, etc.

After evaporation of the solvent, the substrate with the attached powder film is put between two planar steel press plates. A separating foil, e.g. aluminum foil, is placed on top of the powder film to prevent adhesion between the press plate and the film. Pressure is applied by using a hydraulic press. Typical pressures for preparation of $TiO_2$ on a PET/ITO plastic foil are 1000–1500 $kg\,cm^{-2}$. As described below a heat treatment of the compressed films improves the performance of the solar cell.

For the counter electrode, we have developed two alternatives; porous carbon or Sb-doped $SnO_2$ [10]. Similar procedures are applied as for the $TiO_2$ film preparation besides the need of a platinization process of the $SnO_2$ particles in order to catalyze the reduction of tri-iodide at the counter electrode.

For our development work of the solar cell we have internally worked with a *baseline* concept. This emphasizes reproducibility in the preparation steps and the so-called baseline cell is the internal reference from which comparison between alternative preparation procedures and different material components are made, constituting the basis for

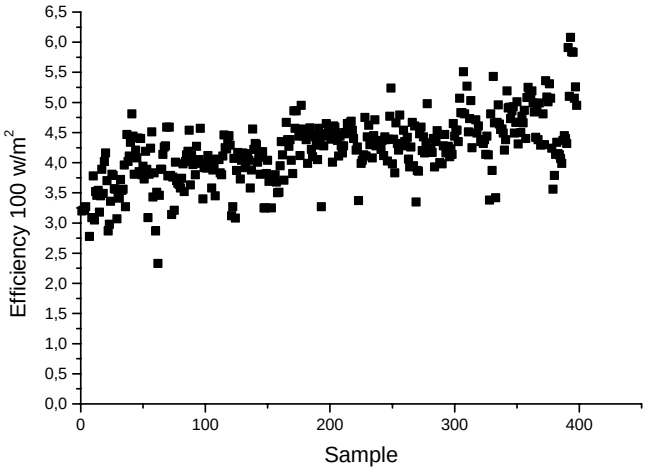


Fig. 1. Efficiency baseline of dye-sensitized solar cells on plastic substrate. The cell is prepared using a dye solution of 0.5 mM *cis*-bis(isothiocyanato)-bis(2,2′-bipyridyl-4,4′-dicarboxylato)ruthenium(II) bis-tetrabutylammonium (normally referred to as N719) dye in ethanol. The electrodes were dye-sensitized by submerging the PET/ITO substrate (supplied by IST, sheet resistance: 60 Ω/square) with the compressed $TiO_2$ film for 2 h in the dye-bath. The counter electrode consisted of the PET/ITO substrate coated with a compressed platinized Sb:$SnO_2$ film (Zelec ECP-3010-XC, supplied by Du Pont. The powder was platinized by mixing 500 μl 5mM $H_2PtCl_6$ in isopropanol with 0.5 g $SnO_2$ and heating the mixture to 375 °C for 10 min. The platinized powder was then crushed and stirred together with 1.5 g ethanol for 12 h). The electrolyte was 0.5 M LiI and 0.05 M $I_2$ and 1-methylbenzimidazole in 3-methoxypropionitrile. The measurements are made with simulated sunlight at 100 W $m^{-2}$ (0.1 sun) using a sulphur lamp (Lightdrive 1000 from Fusion Lightning). The efficiency values are calibrated to correspond to the normal solar spectrum.

our optimization work. If a modification of a preparation step, or an adjusted composition of the chemical solutions, or the use of a new component, etc. give a better cell efficiency compared to the baseline this procedure or component is implemented into the baseline and we have a new internal reference cell to compare with. The development of our baseline activities for flexible plastic DSC is given in Fig. 1. A slight but steady progress in the efficiencies obtained can be observed. The present status of the baseline, monitored at 0.1 sun, is an efficiency of 4.9 ± 0.5%, with a short circuit current ($I_{SC}$) of 1.2 ± 0.1 mA $cm^{-2}$, an open circuit voltage ($V_{OC}$) of 0.65 ± 0.02 V and a fill factor (FF) of 0.65 ± 0.03. The record efficiency value is 6.1%.

There are two main obstacles for the use of plastic DSCs for solar energy applications. Firstly, the plastic substrates have too high resistance in the ITO layer to permit a linearity of the photocurrent up to 1 sun (1000 W $m^{-2}$). The efficiency we obtain for plastic cells at 1 sun is 2–3%. Secondly, the baseline cells described above are not stable. This is due to evaporation of the electrolyte through the permeable plastic substrate. The plastic substrate is also permeable to components in the external environment, for example water and oxygen, which may cause degradation of the cell. Further development of flexible DSC should then focus on development of water tolerant dyes and electrolytes, low-volatile electrolytes and plastic substrates with low resistant conducting layers (<10 Ω/square) and with good barriers towards permeation of water, oxygen and electrolyte. Recently, Haque et al. reported on flexible dye-sensitized solar cells based on pressed $TiO_2$ modified with an ultra-thin $Al_2O_3$ coating. In combination with a solid polymer electrolyte a remarkable efficiency (5.3% at 0.1 sun) and stability (15% decrease after 80 h at 0.2 sun illumination) was achieved [15].

### *2.2. Interconnects compatible with a continuous production process*

In order to minimize internal resistive losses in a solar cell module with an area of several $cm^2$ or larger interconnects must be applied. Interconnects can be applied as current collectors or in a series connection. For a solar cell, such as DSC, which is based on an electrolyte with corrosive components, the interconnects must withstand chemical deterioration. Other criteria for an interconnect technology to be used in plastic DSC modules and being compatible with an inexpensive continuous production process are no or reduced need for high temperature or vacuum environment, no need for masking and comparatively expensive process equipment. Furthermore, a chemical protection of the conducting interconnect wire, as well as a separating barrier between adjacent cells in a multi-cell assembly (module), should be provided at the same time as the electrical connection is established. Fig. 2 shows schematically an interconnect technology that fulfills these criteria [16]. The insulated wire used for electric connections consists of a 0.1 mm spun metal wire coated with a 50 μm thick layer of Surlyn thermoplastic. The metal core consists of seven spun 40 μm thick copper strands.

The conducting ITO layers on the plastic substrates are alternatively on the upper and lower substrate removed by mechanical scribing where the electric interconnects will be positioned. The working and counter electrodes are prepared by the compression technique. To make space for the electric interconnects the compressed oxide films are

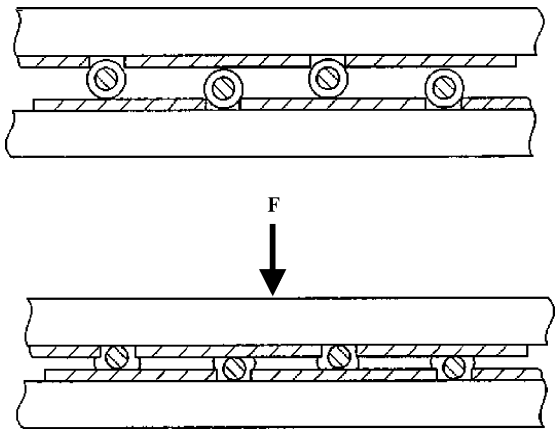


Fig. 2. Schematics of the metal wires coated with a thermoplastic used for interconnects.

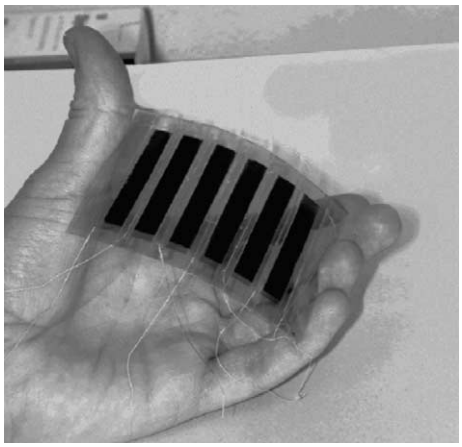

Fig. 3. An interconnected plastic DSC module.

mechanically removed. The whole assembly consisting of the working electrode with deposited $TiO_2$ film, insulated metal wires and the counter electrode with deposited $SnO_2$ film, is compressed. When pressure is applied, the plastic insulation of the wires is deformed according to Fig. 2. For plastic substrates it is preferable to add a step of pre-compression of the wires so that the plastic deformation on the wires is already in place before the whole DSC module is assembled and compressed. Heat treatment of the assembly is necessary (120–130 °C for a few minutes) in order to melt the thermoplastic wire coating. The compression and heat treatment to assemble the plastic DSC module can be performed in a conventional lamination machine. When the insulation is cooled down to room temperature, a protecting plastic barrier is formed between the metal wire and the cell compartment. The plastic barrier also works as a glue between the upper and lower substrates improving the strength of the device. In Fig. 3 we show a picture of an interconnected plastic DSC module with six interconnected cells (total area of 16 $cm^2$). The efficiency is 2.6% (0.1 sun) and at indoor light (200 lx) the output is $V_{OC} = 3$ V, $I_{SC} = 42\ \mu$A and FF = 0.56.

### 2.3. Plastic DSC for indoor applications

For outdoor solar power application, the DSC cells based on plastic cells is in its infancy and not competitive with other photovoltaic technologies. A shortcut to reach the market has therefore been to focus initially on indoor applications where parameters like efficiency and durability may not be as harsh as for outdoor applications. The key feature for plastic DSC is that it is a *flexible* device. This means that it can be uniquely designed for the specific product, in for example shape and colors. This may enable a market entry through new niche markets, in particular, in combination with emerging technologies for autonomous systems (wireless communication) and in packaging.

A flexible DSC on PET substrates suited for indoor environment has been developed. The mesoporous films of $TiO_2$ were produced by compression. The counter-electrode consisted of pressed platinized $SnO_2$ powder and the cells were sealed with Surlyn® hot melt foil. As for the electrolyte 0.5 M NaI,/0.05 M $I_2$ dissolved in polyethyleneglycol was applied together with 1-methylbenzimidazole as an additive. Cells with this configuration were tested under indoor conditions (250 lx, fluorescent light, 30 °C, UV-filter). The results are plotted in Fig. 4 and can be summarized as follows: up to approximately 5000 h, no decrease in the power output occurs. Later, a decrease occurs, which is mainly related to a loss in fill factor and short-circuit current. The voltage on the other side is maintained over the whole period of time

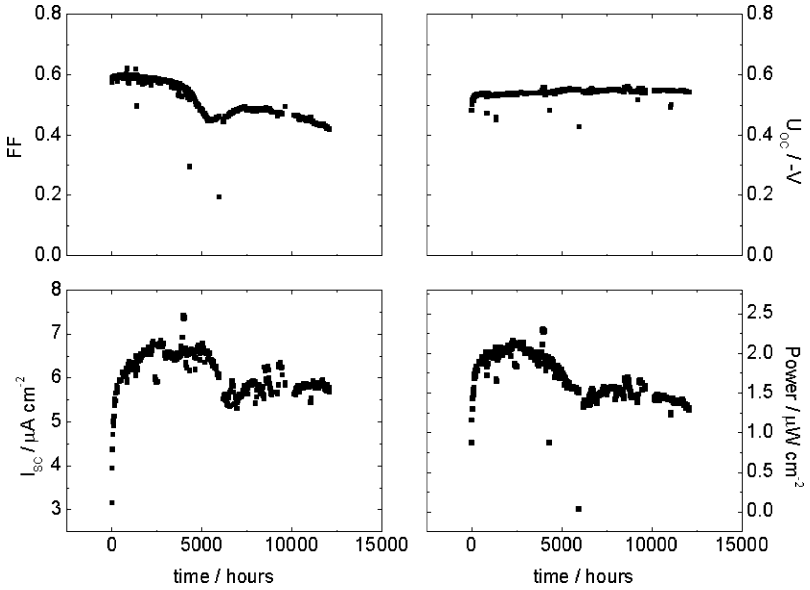


Fig. 4. Performance as a function of time for a DSC on PET substrate (light intensity: 250 lx; DSC: *cis*-Ru (dcbpy)$_2$(SCN)$_2$, 0.5 M NaI, 0.05 M $I_2$, 1-methylbenzimidazole in polymeric solvent).

(almost 1.5 years at continuous illumination). The results demonstrate a sufficient stability for plastic DSC that can be explored for different types of indoor applications.

## 3. Analysis of dye-sensitized solar cells using a system approach

### 3.1. Concept

The internal losses of state-of-the-art DSC correspond to a potential loss of more than 0.5 V. The 'hunt-for-the-half-volt' is our concept to capture this loss and improve the overall efficiency. The concept goes through four sequential steps: (i) identification of the main internal losses; (ii) identification of problems associated with the optimization; (iii) implementation of a strategy for the development of new improved materials; (iv) optimization of new material components in complete DSC devices. An important criterion for the hunt-for-the-half-volt is that the production of the materials is possible to scale up and that the resulting solar modules can be produced in a cost effective way. The main challenge is that the DSC is a complex highly interacting molecular system and the task is to find the optimal way for the different material components to cooperate in the 3D structure or 4D structure since the kinetics of the different electron transfer processes also needs to be well balanced. This calls for a system approach and the development of measurement techniques that allow us to study the internal processes on complete DSC system under relevant conditions. This approach and what we call the 'toolbox' concept is described in the following.

The DSC is a good example of a system where the overall function is not simply the sum of the functions of the separate components. Nanoparticles of $TiO_2$ are extremely poor electron conductors. The $Ru(dcbpy)_2(NCS)_2$ dye is unstable upon illumination in solution. However, when these components are assembled in a dye-sensitized solar cell, the mesoporous $TiO_2$ film becomes a suitable electron acceptor and conductor, and the dye can be stable for many years of illumination. In order to fully understand the DSC and the complex interaction of its components, it will be essential to study the complete solar cell, rather than the separate components.

We have chosen and developed a number of non-destructive analysis techniques that together form the so-called toolbox for dye-sensitized solar cells. By combining the results of the different techniques, we will be able to analyze the limitations/problems of individual cells. The main goals with the toolbox concept are: (i) to measure internal processes on complete DSC devices under normal solar light conditions; (ii) to analyze problems associated with stability and reproducibility; and (iii) to optimize new material components.

Currently, the following techniques are included in this toolbox:

- Photocurrent transients.
- Photovoltage transients.
- Intensity-modulated photocurrent spectroscopy (IMPS).
- Intensity-modulated photovoltage spectroscopy (IMVS).
- Impedance spectroscopy.
- Photo-induced absorption (PIA) spectroscopy.

In addition, information on complete devices will be obtained from conventional methods, such as UV-Vis spectroscopy, IV characterization (under illumination/dark) and photocurrent action spectra (IPCE).

These methods give information on, for example:

| | |
|---|---|
| • Loss mechanisms | -Lifetime of the electrons in the $TiO_2$.<br>-Lifetime of intermediate species in the electrolyte.<br>-Built-up photovoltage in the system during operation.<br>-Built-up concentration of electrons in the $TiO_2$. |
| • Degradation mechanisms | -Lifetime of dye.<br>-Appearance of chemical species related to degradation.<br>-Appearance of loss reactions during accelerated stability tests. |
| • Transport properties | -Transport time for the electrons related to an effective diffusion coefficient.<br>-Determination of transport parameters such as the effective diffusion coefficient, charge mobilities, internal series and shunt resistances. |

We use the following two examples to illustrate the usefulness of some of the above mentioned toolbox techniques.

### 3.2. Effect of pressure and heat-treatment on dye-sensitized solar cells based on compressed $TiO_2$ films

A series of compressed $TiO_2$ films was prepared on transparent conducting oxide (TCO)-coated glass substrates using different pressure. After storage under ambient conditions for 3 weeks, half of the films were dye-sensitized, while the other half were given a heat treatment at 570 °C before dye adsorption. All cells had a similar $TiO_2$ film thickness and dye content. The characteristics of the resulting dye-sensitized solar cells are presented in Table 1. It is clear that cells without heat treatment have a significantly lower efficiency and short-circuit current. In an earlier study it was found that heat treatment after compression of the films did

Table 1
Solar cell characteristics of dye-sensitized solar cells with compressed $TiO_2$ films[a]

| Pressure ($kg\,cm^{-2}$) | Heat treatment | Efficiency (%) 0.1 sun; 1 sun | $V_{OC}$ (V) 0.1 sun; 1 sun | $J_{SC}$ ($mA\,cm^{-2}$) 0.1 sun; 1 sun | Fill factor 0.1 sun; 1 sun |
|---|---|---|---|---|---|
| 570 | – | 2.8; 2.8 | 0.63; 0.70 | 0.57; 5.9 | 0.72; 0.69 |
| 950 | – | 3.3; 3.9 | 0.63; 0.71 | 0.72; 7.2 | 0.74; 0.69 |
| 1900 | – | 3.5; 3.8 | 0.61; 0.68 | 0.79; 7.5 | 0.73; 0.67 |
| 570 | 570 °C, 0.5 h | 5.3; 5.3 | 0.62; 0.71 | 1.17; 11.9 | 0.73; 0.62 |
| 950 | 570 °C, 0.5 h | 5.2; 5.2 | 0.63; 0.72 | 1.16; 11.8 | 0.72; 0.61 |
| 1900 | 570 °C, 0.5 h | 5.0; 4.9 | 0.63; 0.73 | 1.09; 10.7 | 0.72; 0.62 |

[a] Average values of ≥2 cells. Nanostructured $TiO_2$ films were prepared by doctor blading an aqueous suspension of 36 wt.% $TiO_2$ powder (Degussa P25) onto conducting glass substrates, followed by compression. Resulting film thickness was 20–25 μm. The N719 dye was adsorbed during 20 h from a 0.5 mM solution in ethanol and rinsed with warm acetonitrile (50 °C). The electrolyte was 0.6 M TBAI, 0.1 M LiI, 0.5 M 4-*tert*-butylpyridine and 0.1 M $I_2$ in acetonitrile. The active area of the solar cells was 4 $cm^2$.

not have a significant effect on the efficiency [11]. Hence, the lower efficiency of the unsintered films must be due to the storage period, during which adsorption of water and other contaminants can take place at the $TiO_2$ surface. Interestingly, unsintered films prepared at the higher pressures (950 and 1900 $kg\,cm^{-2}$) gave better results than those prepared at 570 $kg\,cm^{-2}$. This may suggest that there was also some degradation of the particle contacts in films prepared at the lower pressure (efficiencies of cells with freshly pressed films do not strongly depend on the pressures applied in this work). If the compressed $TiO_2$ films are given a heat treatment, there is little effect of used pressure on the efficiency.

The IV curves of the dye-sensitized solar cell are well fitted using a 1-diode model that includes resistive losses:

$$V = \frac{mkT}{e} \ln\left(\frac{I_{inj} - I}{I_o} - \frac{V + IR_s}{I_o R_p} + 1\right) - IR_s, \quad (1)$$

where $V$ is voltage, $m$ the diode quality factor, $I$ the current, $I_{inj}$ the injected electron current, $I_0$ the exchange current, $R_s$ the series resistance and $R_p$ the parallel (or shunt) resistance. The characteristics of one cell ($P = 570\,kg\,cm^{-2}$, heated) were analyzed in detail as function of light intensity. The diode quality factor $m$ was found to be 1.6, independent of light intensity. This factor can also be determined from the slope of a plot of $V_{OC}$ versus $\log(J_{SC})$. In this way, $m$ was determined to be 1.5, which is in good agreement.

From the IV-fits, $R_s$ was found to be 2.5 Ω. As the active area is 4 $cm^2$, the series resistance is 10 Ω $cm^2$. At a current density of 10 $mA\,cm^{-2}$, $R_s$ gives a voltage loss of 100 mV. This explains the observed decrease in fill factor at 1 sun illumination. The series resistance contains contributions of the TCO substrates, the charge-transfer reaction at the counter electrode, and of electronic and ionic transport in the nanostructured solar cell. The TCO contribution can be approximated from the sheet resistance and geometrical considerations. The cell has a stripe-like active area of 5 cm × 0.8 cm. There are two current collectors parallel to its length, one on the photoelectrode and one on the counter electrode. Both are located 0.15 cm away from the active area. The sheet resistance of the TCO is 8 Ω/square. Current generated in the photoelectrode has to pass on average 0.4 + 0.15 = 0.55 cm through the TCO to the current collector. The encountered resistance will be (0.55/5) × 8 = 0.88 Ω. The same is true for the counter electrode, so that the total series resistance due to the TCO is expected to be 1.76 Ω. Hence, about 0.74 Ω (or 3 Ω $cm^2$) of the series resistance is due to charge-transfer resistance and electron/ion transport resistance.

The parallel resistance depends strongly on light intensity: $R_p$ is 13 kΩ at 0.1 sun, and 1.3 kΩ at 1 sun. The loss mechanism that is related to $R_p$ is probably a recombination process other than that modeled by the diode ($2e^- + I_3^- \rightarrow 3I^-$). Recombination of electrons with oxidized dye molecules, or with photogenerated $I_2^-$ intermediates are possible candidates.

In intensity-modulated photocurrent and photovoltage spectroscopy, a small sinusoidal light modulation is superimposed onto a constant bias light. The amplitude and phase of the resulting modulated current or voltage is measured as function of the modulation frequency. These methods have successfully been applied to dye-sensitized solar cells [17–20]. The IMPS and IMVS response of a series of DSCs based on pressed $TiO_2$ films was measured. A single time constant was extracted from the data ($\tau_{IMPS}$, $\tau_{IMVS}$) and results are shown in Table 2. $\tau_{IMPS}$ does not differ much between samples prepared with different pressures and with or without heat treatment. $\tau_{IMVS}$, however, is about two times larger for the heated samples. $\tau_{IMVS}$ corresponds to

Table 2
Intensity-modulated photocurrent (photovoltage) spectroscopy time constants of dye-sensitized solar cells with compressed $TiO_2$ films ($\tau_{IMPS}$ and $\tau_{IMVS}$, respectively) (bias light intensity: 1/4 sun[b])

| Pressure ($kg\,cm^{-2}$) | Heat treatment | $\tau_{IMPS}$; $\tau_{CC}$ ($10^{-3}$ s) | $\tau_{IMVS}$ ($10^{-3}$ s) | $\eta_{CC}$ |
|---|---|---|---|---|
| 570 | – | 14; 26 | 32 | 0.57 |
| 950 | – | 11; 24 | 20 | 0.46 |
| 1900 | – | 11; 23 | 21 | 0.49 |
| 570 | 570 °C, 0.5 h | 12; 16 | 45 | 0.74 |
| 950 | 570 °C, 0.5 h | 9.1; 11 | 62 | 0.85 |
| 1900 | 570 °C, 0.5 h | – | – | – |

[b] Modulated light was provided by a red light emitting diode (650 nm, Hewlett-Packard HLMP4101), and white bias light by a halogen lamp. The IMPS response was measured as a voltage across a 10 Ω resistor using a Stanford Research SRS830 lock-in amplifier.

the lifetime of the electrons in the $TiO_2$ under open-circuit conditions. It is not unexpected that the unheated samples show a smaller electron lifetime, as the adsorption of impurities at the $TiO_2$ surface during the storage period may promote recombination of the electrons.

$\tau_{IMPS}$ contains contributions of the electron transport time and the electron lifetime at short circuit conditions. The charge collection time can be approximated as follows: ${\tau_{CC}}^{-1} = {\tau_{IMPS}}^{-1} - {\tau_{IMVS}}^{-1}$ [20]. An assumption that is made here is that the electron lifetime is equal in open and closed circuit conditions. The results are shown in Table 2. There is a large difference in the charge collection time between the cells with and without heat treatment. In the latter the electron transport is about two times slower. The heating treatment is likely to improve the contacts between the $TiO_2$ particles. This suggests that the crossing of the grain boundaries is a rate-limiting step in the electron transport in dye-sensitized solar cells.

From the IMPS and IMVS results, a charge collection efficiency, $\eta_{CC}$, can be calculated as follows: $\eta_{CC} = 1 - (\tau_{IMPS}/\tau_{IMVS})$ [20]. Again it is assumed that the electron lifetime is equal in open and closed circuit conditions. For the heat-treated solar cells the charge collection efficiency is about 80% (see Table 2), i.e. 20% of the photogenerated electrons in the $TiO_2$ are lost due to recombination during the transport to the TCO substrate. Without the heat treatment, $\eta_{CC}$ is reduced to 50%. This observation agrees with the lower short-circuit photocurrents (see Table 1).

### 3.3. Photo-induced absorption spectroscopy of complete dye-sensitized solar cells

Photo-induced absorption (PIA) spectroscopy can give useful spectral and kinetic information on the dye-sensitized solar cell [21]. By using frequency-modulated excitation and lock-in detection, we were able to monitor very small absorption changes in the dye-sensitized solar cell, while using conditions that are similar to typical solar cell operating conditions. The excitation intensity was kept low (<1 sun).

An example of a PIA spectrum of a dye-sensitized solar cell is given in Fig. 5a. In order to obtain a good spectral resolution, no iodine was added to the electrolyte and microscope glass rather than TCO-glass was used as substrate. Similar spectra, however, were recorded using actual cells. Absorption peaks are observed at 390, 520 and 860 nm, while a bleach is observed at 570 nm. Upon illumination, electrons are injected from excited dye molecules ($D^*$) into the nanostructured $TiO_2$ (reaction R1). The oxidized dye molecules ($D^+$) are reduced by iodide (R2). The proposed reaction mechanism is as follows:

$$D^* \rightarrow D^+ + e^-(TiO_2) \quad \text{(R1)}$$

$$D^+ + 2\,I^- \rightarrow I_2^- \quad \text{(R2)}$$

$$2\,I_2^- \rightarrow I^- + I_3^- \quad \text{(R3)}$$

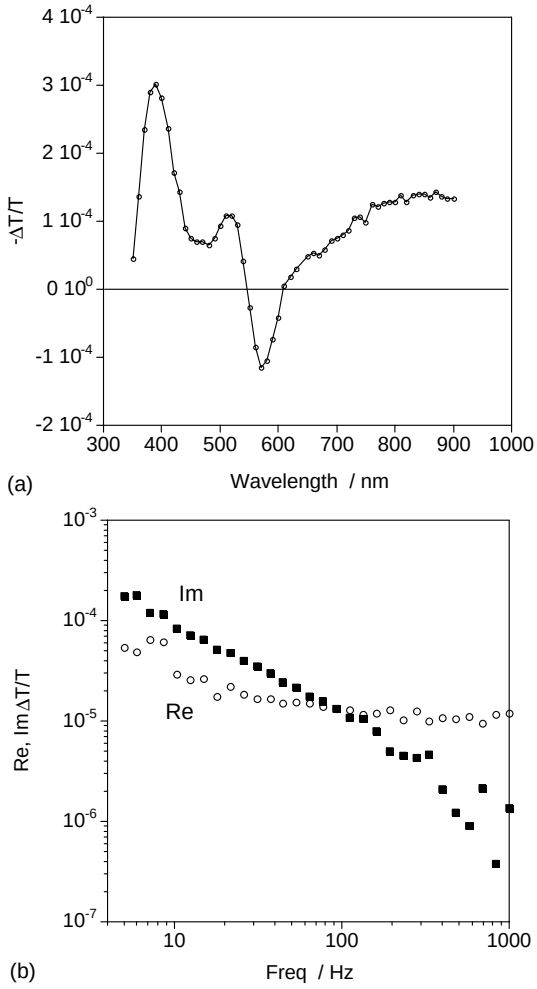


Fig. 5. (a) PIA spectrum of $Ru(dcbpy)_2(NCS)_2$-sensitized nanostructured $TiO_2$ in 0.5 M LiI in propylene carbonate. The PIA system identical to that described in [21], except that a diode laser is used for excitation (modulation frequency 7 Hz). (b) Modulation frequency dependence of the real (in-phase) and imaginary (90° out-of-phase) $\Delta T/T$ signals at $\lambda = 570$ nm.

The importance of the iodine radical anion $I_2^-$ in dye-sensitized solar cells was recently recognized in two independent time-resolved spectroscopic studies [22,23]. In the PIA spectrum, recorded at low modulation frequency (7 Hz) we can expect to see electrons in the $TiO_2$, the iodine radical anion $I_2^-$ and triiodide. Furthermore, it might be possible to see a small contribution of dye molecules in the oxidized state ($D^+$). The $I_2^-$ intermediate has absorption peaks at 390 and 760 nm in aqueous solution [24]. Triiodide absorbs light at wavelengths below ~600 nm in propylene carbonate, with a peak at 363 nm, while iodine has a (much weaker) absorption peak at 462 nm [25]. Electrons in the $TiO_2$ give rise to a broad, featureless absorption at wavelengths exceeding 400 nm [26]. In the PIA spectrum the peak at 390 nm can be attributed to $I_2^-$ and $I_3^-$. The 520 nm peak appears to be due to iodine, which is possibly formed as an intermediate in reaction R3. The broad absorption at

wavelengths higher than 700 nm (maximum at ~860 nm) can be attributed to $I_2^-$ and electrons in $TiO_2$.

Finally, the bleach at 570 nm must be attributed to oxidized dye molecules. No other component in the cell is expected to give a bleach upon illumination except for the dye. At this wavelength, the absorption by $I_2^-$ and $I_3^-$ is negligible, while electrons in $TiO_2$ have a rather small extinction coefficient. Oxidized dye molecules ($D^+$: $Ru^{III}(dcbpy)_2(NCS)_2$) show a strong decrease in absorption below 600 nm (peaks at 540 and 440 nm) and an increase at higher wavelengths (peak at 860 nm), in comparison with the ground-state absorption of D. The magnitude of the PIA signal in the low-frequency (near steady-state) limit $(\Delta T/T)_{SS}$ for a first order reaction is given by:

$$\left(-\frac{\Delta T}{T}\right)_{SS} = \ln(10) \times \frac{I_0}{N_A}\left(1 - e^{-\Gamma_D \varepsilon_D}\right)\phi\varepsilon_L\tau \qquad (2)$$

where $I_0$ is the incident photon flux, $N_A$ the Avogadro constant, $\Gamma_D$ and $\varepsilon_D$ the coverage and the absorption coefficient of the dye, respectively, $\phi$ the quantum efficiency for photoinduced generation of species L, $\varepsilon_L$ the differential absorption coefficient of this species with respect to D, and $\tau$ the lifetime of L. The lifetime of D* is about $10^{-12}$ s due to ultrafast electron injection, while that of electron in the $TiO_2$ is in the order of $10^{-2}$ s. Taking into account that $\varepsilon$ for electrons in $TiO_2$ is about 10 times smaller than that of D*, the resulting PIA signal at low-frequencies of electrons will be about $10^9$ times stronger than that of D*. Consequently, the contribution of D* cannot be seen. The lifetime of $D^+$ in the presence of a high concentration of iodide is reported to be 0.1 μs [27] to 10 μs [28]. Using similar argumentation, the $D^+$ signal will be $10^{-4}$ to $10^{-2}$ times smaller than the electron signal: a small contribution to the PIA spectrum may be seen. However, the strong bleaching feature observed in Fig. 5a is not expected.

Fig. 5b shows the frequency dependence of the 570 nm PIA signal. As expected, the magnitude of the signals increases with decreasing modulation frequency. Interestingly, the real part has a non-zero value at high frequencies. This offset corresponds to the steady-state value $(\Delta T/T)_{SS}$ of a fast reaction. By using Eq. (2), an estimate can be made for the lifetime of this reaction: $\tau \approx 60$ μs. This is a reasonable value for the regeneration of the oxidized dye by iodide in propylene carbonate (R2).

From the frequency dependence of the PIA signals at 570 nm the lifetime of the slower reaction is determined to be 0.13 s. This is similar to the lifetime observed for the dye adsorbed at $TiO_2$ in the absence of iodide. We think that the slow reaction is due to dye molecules that are not in contact with iodide. Excitation of these dye molecules would result in electron injection into $TiO_2$, but the only regeneration mechanism for these molecules is the back-reaction with the injected electrons. Dye molecules that have no access to iodide could occur in pores with trapped air instead of electrolyte. Alternatively, dye trapped in extremely narrow channels may be excluded from an iodide supply. From the PIA results we estimate that about 1% of dye is non-active.

## 4. Some views on future work

The coming generation of solar cell technologies must be based on thin film technologies with efficiencies above 10%, similar lifetime expectancies as the conventional silicon cells and having a larger potential for cost reduction in production technology than Si-based solar cells. For areas larger than 1 $cm^2$ the record efficiency for DSC is 8.18% [29]. Regarding stability, DSC cells have gone through the standardized acceleration test for silicon cells at 6% efficiency. For flexible DSC technologies there is still a quantum leap to be made before sufficiently stable, efficient and large cells in modules can be made.

From the literature and our own investigations [30] we conclude that the two main internal losses are the ones being schematically drawn in Fig. 6. The first step represents a potential loss of about 0.6 V between the electrolyte redox potential and the oxidized level of the dye. The second step is loss of electrons in the $TiO_2$ to the electrolyte, a step that is largely dependent on the concentration of electrons in the $TiO_2$, i.e. it depends on light intensity. An interesting question in step 1, which has not been thoroughly discussed, is how much of the potential loss that can be captured, i.e. what is the minimum driving force of the step needed while still having sufficiently fast kinetics (ns time scale).

The *potential* of DSC lies in the fact that components with better individual characteristics than the ones used in the state-of-the-art device have been developed. The *problem* is that the full potential of these components have not been possible to utilize in a complete DSC device. We therefore need to take the new, and from the individual characteristics, better components and learn better how these components interact within the system and identify the problems associated with the optimization of the DSC system as a whole. Examples of these components are:

1. Oxide nanofiber structures: Improving the charge transport through the mesoporous oxide layer will reduce the

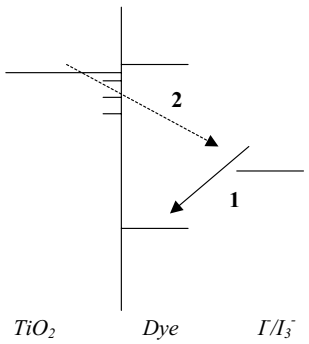


Fig. 6. A schematic diagram showing the two main internal losses in state-of-the-art DSC.

electron losses in the oxide to the electrolyte (step 2 in Fig. 6). The optimal electronic charge transport is through nanofibers, giving a directed transport of the electrons to the conducting back contact [31].

2. Dyes with optimal spectral properties—so called 'Black dyes': Dyes with absorption thresholds longer than 900 nm exist today [32,33]. An optimal use of these dyes will improve the cell efficiencies significantly.
3. Solid-state electrolyte: Copper thiocyanate (CuSCN) has been reported to fulfill basically all the requirements one can have on the electrolyte, besides a question mark for the stability issue. The problem with CuSCN has been in the processing, that is to fill the nanoporous $TiO_2$ efficiently to make a good interface between the $TiO_2$/dye/CuSCN components in the 3D system.

Another feature in the directions to improve the performance of the DSC technology is the progress of the control of the $TiO_2$–dye–electrolyte interface by the development of well ordered mesoporous $TiO_2$ films, core–shell structures of the oxide particles, self-assembly of the dye monolayer, etc. (see, for example [34]).

An important and powerful optimization tool for the development of new materials to improve the DSC technology is to apply statistical methods. It will therefore be important to develop sample preparation procedures making it possible to prepare several solar cells in one step and on one substrate. The use of such a 'master plate' will create a solid statistical basis for optimization, through for example multivariable analysis, and for studies of degradation mechanisms.

## Acknowledgements

Prof. Michael Grätzel and his co-workers are gratefully acknowledged for support and fruitful collaborations over the years. We thank Energy Research Center of the Netherlands (ECN) for support in the preparation of samples described in Section 3.2. This work has been supported by the Swedish National Energy Administration (Energimyndigheten), the Swedish Foundation for Strategic Environmental Research (MISTRA) and the PSO-project under ELTRA project number 3629 (Denmark).

## References

[1] B. O'Regan, M. Grätzel, Nature (London) 353 (1991) 737.
[2] M.K. Nazeeruddin, A. Kay, I. Rodicio, R. Humphry-Baker, E. Müller, P. Liska, N. Vlachopoulos, M. Grätzel, J. Am. Chem. Soc. 115 (1993) 6382.
[3] A. Hagfeldt, M. Grätzel, Acc. Chem. Res. 33 (2000) 269.
[4] P. Wang, S.K. Zakeeruddin, J.E. Moser, M.K. Nazeeruddin, T. Sekigushi, M. Grätzel, Nat. Mater. 2 (2003) 402.
[5] A. Hagfeldt, L. Walder, M. Grätzel, Proc. SPIE-Int. Soc. Opt. Eng. 2531 (1995).
[6] P. Bonhote, E. Gogniat, F. Campus, L. Walder, M. Grätzel, Displays 20 (1999) 137.
[7] S.Y. Huang, L. Kavan, I. Exnar, M. Grätzel, J. Electrochem. Soc. 142 (1995) L142.
[8] K. Vinodgopal, S. Hotchandani, P.V. Kamat, J. Phys. Chem 97 (1993) 9040.
[9] H. Lindström, S. Södergren, S.-E. Lindquist, A. Hagfeldt, Method for Manufacturing Nanostructured Thin Film Electrodes, International Patent Application Nr. PCT/SE00/01060. Filed: May 25, 2000.
[10] H. Lindström, A. Holmberg, E. Magnusson, S.-E. Lindquist, L. Malmqvist, A. Hagfeldt, Nano Lett. 1 (2001) 97.
[11] H. Lindström, E. Magnusson, A. Holmberg, S. Södergren, S.-E. Lindquist, A. Hagfeldt, Sol. Energy Mater. Sol. Cells 73 (2002) 91.
[12] F. Pichot, J.R. Pitts, B.A. Gregg, Langmuir 16 (2000) 5626.
[13] R. Gaudiana, J. Macromol. Sci.—Pure Appl. Chem. A39 (2002) 1259.
[14] D. Zhang, T. Yoshida, H. Minoura, Adv. Mater. 15 (2003) 814.
[15] S.A. Haque, E. Palomares, H.M. Upadhyaya, L. Otley, R.J. Potter, A.B. Holmes, J.R. Durrant, Chem. Commun. (2003) 3008.
[16] H. Lindström, S. Södergren, S.-E. Lindquist, A. Hagfeldt, Electric Connection of Cells, International Patent Application Nr. PCT/SE00/00003. Filed: January 3, 2000.
[17] L. Dloczik, O. Ileperuma, I. Lauermann, L. Peter, E. Ponomarev, G. Redmond, N. Shaw, I. Uhlendorf, J. Phys. Chem. B 101 (1997) 10281.
[18] G. Schlichthörl, S.Y. Huang, J. Sprague, A.J. Frank, J. Phys. Chem. B 101 (1997) 8139.
[19] A.C. Fisher, L.M. Peter, E.A. Ponomarev, A.B. Walker, K.G.U. Wijayantha, J. Phys. Chem. B 104 (2000) 949.
[20] J. van de Lagemaat, N.G. Park, A.J. Frank, J. Phys. Chem. B 104 (2000) 2044.
[21] G. Boschloo, A. Hagfeldt, Chem. Phys. Lett. 370 (2003) 381.
[22] I. Montanari, J. Nelson, J.R. Durrant, J. Phys. Chem. B 106 (2002) 12203.
[23] C. Bauer, G. Boschloo, E. Mukhtar, A. Hagfeldt, J. Phys. Chem. B 106 (2002) 12693.
[24] R. Devonshire, J.J. Weiss, J. Phys. Chem. 72 (1968) 3015.
[25] K.J. Hanson, C.W. Tobias, J. Electrochem. Soc 134 (1987) 2204.
[26] B. O'Regan, M. Grätzel, D. Fitzmaurice, Chem. Phys. Lett. 183 (1991) 89.
[27] S.A. Haque, Y. Tachibana, D.R. Klug, J.R. Durrant, J. Phys. Chem. B 102 (1998) 1745.
[28] S. Pelet, J.-E. Moser, M. Grätzel, J. Phys. Chem. B 104 (2000) 1791.
[29] A. Hinsch, J. Kroon, R. Kern, R. Sasrawan, A. Meyer, I. Uhlendorf, in: Proceedings of the 17th European Photovoltaic Solar Energy Conference, Munich, 2001, p. 51.
[30] G. Boschloo, H. Lindström, E. Magnusson, A. Holmberg, A. Hagfeldt, J. Photochem. Photobiol. A: Chem. 148 (2002) 11.
[31] N. Beermann, L. Vayssieres, S.-E. Lindquist, A. Hagfeldt, J. Electrochem. Soc. 147 (2000) 2456.
[32] M.K. Nazeeruddin, P. Péchy, T. Renouard, S.M. Zakeeruddin, R. Humphry-Baker, P. Comte, P. Liska, L. Cevey, E. Costa, V. Shklover, L. Spiccia, G.B. Deacon, C.A. Bignozzi, M. Grätzel, J. Am. Chem. Soc. 123 (2001) 1613.
[33] A. Islam, H. Sugihara, M. Yanagida, K. Hara, G. Fujihashi, Y. Tachibana, R. Katoh, S. Murata, H. Arakawa, New J. Chem. 26 (2002) 966.
[34] M. Grätzel, J. Photochem. Photobiol. C: Photochem. Rev. 4 (2003) 145.